

Soft Lithography Using Acryloxy Perfluoropolyether Composite Stamps

Tu T. Truong,[†] Rongsheng Lin,[†] Seokwoo Jeon,[†] Hee Hyun Lee,[†] Joana Maria,[†]
Anshu Gaur,[†] Feng Hua,[‡] Ines Meinel,[§] and John A. Rogers^{*,†}

Department of Chemistry, Department of Materials Science and Engineering, Department of Electrical and Computer Engineering, Beckman Institute and Frederick Seitz Materials Research Laboratory, University of Illinois at Urbana–Champaign, Urbana, Illinois 61801, Department of Electrical and Computer Engineering, Clarkson University, Potsdam, New York 13699, and Mitsubishi Chemical, Research and Innovation Center, Goleta, California 93117

Received October 10, 2006. In Final Form: December 5, 2006

This paper describes composite patterning elements that use a commercially available acryloxy perfluoropolyether (a-PFPE) in various soft lithographic techniques, including microcontact printing, nanotransfer printing, phase-shift optical lithography, proximity field nanopatterning, molecular scale soft nanoimprinting, and solvent assisted micromolding. The a-PFPE material, which is similar to a methacryloxy PFPE (PFPE-DMA) reported recently, offers a combination of high modulus (10.5 MPa), low surface energy (18.5 mNm⁻¹), chemical inertness, and resistance to solvent induced swelling that make it useful for producing high fidelity patterns with these soft lithographic methods. The results are comparable to, and in some cases even better than, those obtained with the more widely explored material, high modulus poly(dimethylsiloxane) (h-PDMS).

Introduction

Soft lithographic methods comprise a collection of techniques that use soft elastomeric stamps, molds, and conformable photomasks as patterning elements. These methods have been applied, mostly in research applications, in areas ranging from photonics and biotechnology to microfluidics and electronics. They are of interest due to their ease of use, flexible patterning capabilities, experimental simplicity, and, in development work for realistic applications, their potential to be low in cost.¹ Although a variety of materials, including polycarbonate resins,² cross-linked novolak based epoxy resins,³ fluoropolymer materials (such as Dupont Teflon AF 2400: a copolymer of 2,2-bistrifluoromethyl-4,5-difluoro-1,3-dioxole (PDD) and tetrafluoroethylene (TFE)),^{4,5} α , ω -methacryloxy functionalized PFPE (PFPE-DMA),⁶ etc. have been used, poly(dimethylsiloxane) (PDMS) represents the most popular choice. PDMS is attractive because (i) its flexible backbone enables accurate replication of relief shapes in the fabrication of the patterning elements, (ii) its low Young's modulus and low surface energy enable conformal contact with surfaces without applied pressure^{7–9} and nondestructive release from patterned structures, (iii) its high degree

of physical toughness and high elongation at break (>150%) lead to robust and rugged patterning elements, and (iv) its commercial availability in bulk quantities at low cost facilitates development work. PDMS elements are easily fabricated and are capable of patterning both flat and curved surfaces,¹⁰ two-dimensional as well as three-dimensional structures,^{11–13} and with resolution that approaches the molecular limit.¹⁴ One of the most commonly used PDMS formulations (Sylgard 184, Dow Corning) has, however, some disadvantages: (i) its low modulus (~1.5 MPa)⁶ limits the fabrication of features with high aspect ratios due to collapse, merging, and buckling of the structures of relief,^{7,15,16} (ii) its surface energy (~25 mN m⁻¹) is not low enough for high fidelity, nondestructive fabrication in certain cases,⁶ (iii) its poor solvent resistance causes the PDMS to swell when exposed to most organic solvents, (iv) its high thermal expansion coefficient (260 $\mu\text{m m}^{-1} \text{ }^\circ\text{C}^{-1}$) and thermal curing process can lead to deformations and distortions during the fabrication or use of the patterning elements, and (v) it is not easy to pattern structures in PDMS by means other than casting and curing against structures of relief.

Several variants of PDMS have been made to improve the resolution and fidelity in soft lithography. For example, Michel et al. developed a PDMS (known as hard PDMS or h-PDMS) with a modulus of ~9 MPa that uses short cross-linkers.¹⁷ Although this material is brittle, it can be used effectively in

[†] University of Illinois at Urbana–Champaign.

[‡] Clarkson University.

[§] Mitsubishi Chemical.

* Author to whom correspondence should be addressed. E-mail: jrogers@uiuc.edu.

(1) Rogers, J. A.; Nuzzo, R. G. *Mater. Today* **2005**, *8*, 50–56.

(2) Pisignano, D.; D'Amone, S.; Gigli, G.; Cingolani, R. *J. Vac. Sci. Technol., B* **2004**, *22*, 1759–1763.

(3) Pfeiffer, K.; Fink, M.; Ahrens, G.; Gruetzner, G.; Reuther, F.; Seekamp, J.; Zankovych, S.; Torres, S. C. M.; Maximov, I.; Beck, M.; Graczyk, M.; Montelius, L.; Schulz, H.; Scheer, H.-C.; Steingrueber, F. *Microelectron. Eng.* **2002**, *61–62*, 393–398.

(4) Khang, D.-Y.; Lee, H. H. *Langmuir* **2004**, *20*, 2445–2448.

(5) Khang, D.-Y.; Kang, H.; Kim, T.-I.; Lee, H. H. *Nano Lett.* **2004**, *4*, 633–637.

(6) Rolland, J. P.; Hagberg, E. C.; Denison, G. M.; Cater, K. R.; DeSimone, J. M. *Angew. Chem. Int. Ed.* **2004**, *43*, 5796–5799.

(7) Huang, Y. G. Y.; Zhou, W. X.; Hsia, K. J.; Menard, E.; Park, J. U.; Rogers, J. A.; Alleyne, A. G. *Langmuir* **2005**, *21*, 8058–8068.

(8) Hsia, K. J.; Huang, Y.; Menard, E.; Park, J.-U.; Zhou, W.; Rogers, J. A.; Fulton, J. M. *Appl. Phys. Lett.* **2005**, *86*, 154106.

(9) Zhou, W.; Huang, Y.; Menard, E.; Aluru, N. R.; Rogers, J. A.; Alleyne, A. G. *Appl. Phys. Lett.* **2005**, *87*, 251925.

(10) Xia, Y.; Whitesides, G. M. *Angew. Chem. Int. Ed.* **1998**, *37*, 550–575.

(11) Gates, B. D.; Xu, Q.; Stewart, M.; Ryan, D.; Willson, C. G.; Whitesides, G. M. *Chem. Rev.* **2005**, *105*, 1171–1196.

(12) Jeon, S.; Malyarchuk, V.; Rogers, J. A.; Wiederrecht, G. P. *Opt. Express* **2006**, *14*, 2300–2308.

(13) Jeon, S.; Park, J.-U.; Cirelli, R.; Yang, S.; Heitzman, C. E.; Braun, P.; Kenis, P. J. A.; Rogers, J. A. *Proc. Natl. Acad. Sci. U.S.A.* **2004**, *101*, 12428–12433.

(14) Hua, F.; Sun, Y.; Gaur, A.; Meitl, M. A.; Bilhaut, L.; Rotkina, L.; Wang, J.; Geil, P.; Shim, M.; Rogers, J. A.; Shim, A. *Nano Lett.* **2004**, *4*, 2467–2471.

(15) Hui, C. Y.; Jagota, A.; Lin, Y. Y.; Kramer, E. J. *Langmuir* **2002**, *18*, 1394–1407.

(16) Odom, T. W.; Love, J. C.; Wolfe, D. B.; Paul, K. E.; Whitesides, G. M. *Langmuir* **2002**, *18*, 5314–5320.

(17) Schmid, H.; Michel, B. *Macromolecules* **2000**, *33*, 3042–3049.

composite stamps that consist of a thin layer of h-PDMS with a thick backing layer of the Sylgard 184 material (known as soft PDMS or s-PDMS).¹⁶ Another photocurable version of PDMS (hv-PDMS, with a modulus of ~ 4 MPa) uses rigid urethane methacrylate cross-linkers.^{18,19} The ability to photocure this material (and, therefore, to photopattern it) is attractive because such a process avoids distortions that can occur during thermal curing based approaches to fabricating the patterning elements. The photopatterning possibility also provides unconventional routes to forming these elements, in ways that can complement the standard casting and curing approach.

DeSimone et al. recently reported the use of photocurable perfluoropolyethers (PFPEs) for microfluidic devices and a type of imprint lithography.^{6,20,21} The reported PFPE, α -, ω -methacryloxy functionalized PFPE (PFPE-DMA), contains two methacryloxy ending groups ($\text{CH}_2=\text{C}(\text{CH}_3)\text{COO}-$) on the fluorinated polyether backbone.⁶ The fluoropolymer, which is liquid at room temperature, can be cross-linked under ultraviolet (UV) light to yield elastomers with an extremely low surface energy ($\sim 12 \text{ mN m}^{-1}$). The reported PFPE has a modulus of ~ 4 MPa,⁶ which is comparatively larger than s-PDMS, similar to the previously reported hv-PDMS, and somewhat less than h-PDMS. A major advantage of PFPE based materials is that they are solvent resistant and chemically robust and therefore swell much less significantly than PDMS when exposed to most organic compounds. This characteristic expands the range of materials that can be patterned effectively. Also, unlike PDMS, PFPEs eliminate the surface functionalization step that is often required to avoid adhesion to oxides (e.g., SiO_2 on Si wafers) during the casting and curing steps used to make the patterning elements. PFPE based stamps have been demonstrated to have the capability of patterning 70 nm features with a precision of ± 1 nm,⁶ imprinting and molding of 1–2 nm diameter carbon nanotubes, as well as dual damascene structures.²¹ PFPEs have also been utilized in a method termed pattern replication in non-wetting templates (PRINT) for the fabrication of micro- and nanoparticles and structured arrays^{22,23} and for the nondestructive measurement and inspection of complex, high-aspect ratio features.²¹

In the work presented here, we explore the use of a commercially available form of PFPE (CN4000 from Sartomer Company, Inc., $\text{MW} = 1000 \text{ g mol}^{-1}$) in a variety of soft lithographic techniques and compare its behavior to h-PDMS. The material is a fluorinated acrylate oligomer with a low surface energy (18.5 mN m^{-1}), low viscosity (60 cps at 25 °C), and low refractive index (1.341) and was originally designed for ultraviolet or electron beam cured coatings and for electronics. This oligomer has the backbone of fluorinated polyether with acryloxy ($\text{CH}_2=\text{CH}-\text{COO}-$) as ending functional groups instead of methacryloxy groups in the reported PFPE-DMA. The material, which we denote as a-PFPE, is cross-linked under UV illumination to form a high modulus elastomer (10.5 MPa). The modulus of a-PFPE is higher than that of the reported PFPE-DMA (4 MPa)⁶ but much smaller than that of the thermoformed rigid fluoromaterial, Dupont Teflon AF2400 (1.6 GPa).^{4,5} As a result, a-PFPE can achieve high fidelity replication while at the same time enabling

good conformal contact with target substrates without substantial applied pressure. We report results obtained by use of this photocured a-PFPE in composite patterning element designs that use backing layers of s-PDMS and other materials. We explore, in particular, a broad range of traditional and newer soft lithographic methods, including microcontact printing (μCP),¹⁰ nanotransfer printing (nTP),²⁴ phase-shift lithography,²⁵ proximity field nanopatterning (PnP),^{12,13} molecular scale soft nanoimprinting,^{14,26} and solvent assisted micromolding (SAMIM).¹⁰ As an application example, we form high-resolution quasi-three-dimensional plasmonic crystals and evaluate their transmission characteristics. We find that, for these soft lithographic techniques, a-PFPE compares favorably with h-PDMS, and that its other features (e.g., resistances to swelling, ability to photocure, etc.), which are similar to those of the previously reported PFPE-DMA, can provide certain new capabilities.

Experimental Procedures

a-PFPE Stamp Fabrication. The a-PFPE formulation used a fluorinated acrylate oligomer, CN4000 (Sartomer Company, Inc., $\text{MW} = 1000 \text{ g mol}^{-1}$), and a photoinitiator (Darocurr 4265, Ciba Specialty Chemicals) (0.5 wt %) consisting of 50% of 2,4,6-trimethylbenzoyl-diphenyl-phosphineoxide and 50% of 2-hydroxy-2-methyl-1-phenyl-propanone. Filtering the mixture through a 0.22 μm syringe filter after mixing for 2 h formed a photocurable liquid resin. For most examples illustrated here, spin casting (4000 rpm for 30 s) formed a thin layer ($\sim 2 \mu\text{m}$ thick) of this photocurable liquid resin on a pattern of a photoresist on a silicon wafer that served as the master for fabricating the patterning elements. Exposing the film to UV light (350–380 nm) from a mercury lamp with an intensity of 4 mW/cm² under nitrogen purge for 2 h cured the material. Casting s-PDMS (Sylgard 184 Silicon Elastomer, Dow Corning) onto the a-PFPE layer and curing it at room temperature for ~ 48 h or at 65 °C for 2 h formed a support layer ($\sim 4 \text{ mm}$ thick) for a composite a-PFPE/s-PDMS structure. Peeling the a-PFPE/s-PDMS off of the master completed the fabrication of the patterning element. In this approach, the a-PFPE is not strongly bonded to the h-PDMS, but the adhesion is sufficient for the patterning procedures described here.

Molecular scale molding experiments used masters that consisted of single walled carbon nanotubes (SWNTs) on SiO_2/Si substrates. In these cases, composite molds that used polyethylene terephthalate (PET) film backings performed better than those that used s-PDMS, possibly due to slight distortions generated in the a-PFPE surface, at molecular length scales, by curing induced shrinkage in the s-PDMS. Fabrication of an a-PFPE/PET mold began with placing a few drops of a liquid a-PFPE mixture onto a SWNT master. Spin casting (3000 rpm for 30 s) a thin film of polyurethane (NOA-73, Norland Optical Adhesives, 1:2 diluted with acetone) onto a PET sheet and pre-curing it under UV light for 3 min formed a layer that promoted adhesion to the a-PFPE. Placing the coated PET on top of the a-PFPE spread the liquid precursor uniformly over the master. Exposing the liquid a-PFPE with UV light from an Hg lamp (350–380 nm) with an intensity of 4 mW/cm² for 2 h in nitrogen purge cured the material. Peeling the supported a-PFPE mold away from the master completed the process.

Physical Characterization. We evaluated the relative modulus and surface energy of thin films of a-PFPE. The modulus was measured on a $\sim 25 \mu\text{m}$ thick layer of PFPE on PET, using a Hysitron TriboIndenter (Hysitron Inc.) and determined according to the test method described previously.²⁷ The instrument was equipped with

(18) Choi, K. M.; Rogers, J. A. *J. Am. Chem. Soc.* **2003**, *125*, 4060–4061.

(19) Choi, K. M. *J. Phys. Chem. B* **2005**, *109*, 21525–21531.

(20) Rolland, J. P.; Van Dam, R. M.; Schorzman, D. A.; Quake, S. R.; DeSimone, J. M. *J. Am. Chem. Soc.* **2004**, *126*, 2322–2323.

(21) Rothrock, G. D.; Maynor, B.; Rolland, J. P.; DeSimone, J. M. *Proc. SPIE-Int. Soc. Opt. Eng.* **2006**, *6152*, 61523.

(22) Rolland, J. P.; Maynor, B. W.; Euliss, L. E.; Exner, A. E.; Denison, G. M.; DeSimone, J. M. *J. Am. Chem. Soc.* **2005**, *127*, 10096–10100.

(23) Wiles, K. B.; Wiles, N. S.; Herlihy, K. P.; Maynor, B. W.; Rolland, J. P.; DeSimone, J. M. *Proc. SPIE-Int. Soc. Opt. Eng.* **2006**, *6151*, 61513.

(24) Menard, E.; Bilhaut, L.; Zaumseil, J.; Rogers, J. A. *Langmuir* **2004**, *20*, 6871–6878.

(25) Maria, J.; Malyarchuk, V.; White, J.; Rogers, J. A. *J. Vac. Sci. Technol., B* **2006**, *24*, 828–835.

(26) Hua, F.; Gaur, A.; Sun, Y.; Word, M.; Jin, N.; Adesida, I.; Shim, M.; Shim, A.; Rogers, J. A. *IEEE Trans. Nanotechnol.* **2006**, *5*, 301–308.

(27) Oliver, W. C.; Pharr, G. M. *J. Mater. Res.* **1992**, *7*, 1564.

a Berkovich diamond indenter to perform indentations on a sample of the elastomeric stamp. For each stamp, at least two sets of 25 indentations to a maximum load of 100 μN were conducted. Any surface effect and interaction with the substrate were minimized by indenting more than 10 times the measured surface roughness, but not more than 10% of the total thickness of the sample. Indentations within each set were 10 μm apart, and the sets were separated by at least 1 mm. The indentations were made using a 5–2–5 load function in which there was 5 s to apply the load, 2 s of hold (under load control closed-loop feedback) to reduce the effect of hysteresis/creep, and then a 5 s unload. The analysis of the load/unload curves for each indentation was performed following the method of Oliver and Pharr to determine the modulus of elasticity.²⁷ Seventy-five percent of the unloaded portion of the curve starting from 5% from the top to 20% from the bottom was used for the calculation to determine the modulus of elasticity. The indenter area function that was required for analysis of the nanoindentation data using this method was calculated using a series of indents in fused silica. Comparison measurements show that a-PFPE has a modulus that is approximately the same as h-PDMS and is 7 times higher than s-PDMS.

The surface energy was evaluated from the measurement of the advancing and receding contact angle of water and methylene iodide on the cured a-PFPE surface, using a video contact angle analyzer, VCA 2500xe (Advanced Surface Technology Products). The contact angle of a liquid on the examined solid surface could be related to the solid surface energy through Young's equation. The advancing angles measured with water and methylene iodide were used with the Harmonic mean approximation to calculate the solid surface energy.

h-PDMS Stamp Fabrication. The formulation for h-PDMS (Gelest, Inc.) can be found elsewhere.¹⁴ Spin casting a prepolymer mixture of this material onto a master at 500 rpm for 30 s, 1000 rpm for 40 s, and 500 rpm for 800 s and baking for 3 min at 65 °C formed a ~ 20 μm thick layer of h-PDMS. Pouring s-PDMS (Sylgard 184, Dow Corning) onto this layer and curing for 2 h at 65 °C formed a ~ 4 mm thick backing. Peeling away the composite h-PDMS/s-PDMS element completed the process.

Linear Polymerization Shrinkage Measurements. Linear polymerization shrinkage measurements were performed with an optical microscope, using procedures described previously.¹⁹ In these measurements, a master with line and space patterns of a photoresist (Shipley 1805, relief depth = 450 nm, line width = 6.3 μm , and periodicity = 9.5 μm) was used. Images of corresponding regions on a-PFPE (2 μm)/s-PDMS (4 mm) and h-PDMS (20 μm)/s-PDMS (4 mm) stamps fabricated from these masters were collected. The shrinkage was determined from the difference in periodicity of the patterns on stamps and the master.

Fabrication of Masters for Phase-Shift Lithography. Masters for phase-shift masks used silicon-on-insulator (SOI) structures, anisotropically etched using a KOH based etchant, as described previously.²⁵ These procedures formed structures consisting of parallel lines and spaces (1–20 μm) with vertical, smooth sidewalls and top and bottom surfaces.

Microcontact Printing. a-PFPE/s-PDMS and h-PDMS/s-PDMS were formed using masters consisting of patterns of photoresists (300 nm to 1 μm dots with a periodicity of 600 nm to 1.6 μm) on silicon wafers. Placing drops of a 1 mM solution of hexadecanethiol (HDT) in ethanol on the a-PFPE/s-PDMS stamps for 5–10 min and blowing off the solvent with a nitrogen gun comprised the inking step. Placing the inked stamps in conformal contact with a 2 nm/20 nm Ti/Au bilayer for 30 s and peeling off the stamp left a patterned self-assembled monolayer (SAM) of HDT on the gold. Etching the printed substrates for ~ 10 min in an etchant of 300 mL of H₂O, 16.8 g of KOH, 1.09 g of K₃[Fe(CN)₆], 0.13 g of K₄[Fe(CN)₆], and 7.4 g of Na₂S₂O₃·5H₂O removed the unprotected gold, yielding patterned structures in the geometry of the relief on the stamps. The microcontact printing process with h-PDMS/s-PDMS stamps was similar to that with a-PFPE/s-PDMS but with slightly different contact and inking times, as described in the main text.

Nanotransfer Printing (nTP). Nanotransfer printing relies on the transfer of thin solid layers of material from the surface of a stamp to a substrate. Here, we explored nTP of gold onto substrates coated with a thin layer of gold. In this case, cold welding facilitates the transfer of gold from the stamp to the substrate. For h-PDMS/s-PDMS stamps, a short treatment of the stamps with oxygen plasma for ~ 4 s followed by deposition of a double layer of Ti/Au (2 nm/20 nm) enabled high yield transfer of largely crack-free patterns, as described previously.²⁴ For a-PFPE/s-PDMS stamps, crack free transferred films could not be obtained using the optimized conditions for h-PDMS/s-PDMS stamps due perhaps to the poor wettability of the a-PFPE surface. Cracks could be reduced, however, by increasing the extent of oxygen plasma treatment (to ~ 30 s) and by using a multilayer stack of metals (Ti/Au/Ti/Au, 8 nm/10 nm/2 nm/10 nm). Transfer of these layers from the stamp to substrate occurred at high yields and easily due to the very weak adhesion of the metal layers to the a-PFPE surface.

Three-Dimensional Nanostructure Fabrication. We used procedures described previously in an optical method for three-dimensional nanofabrication, known as proximity field nanopatterning (PnP).¹³ In this procedure, h-PDMS or a-PFPE phase masks with relief features that have lateral dimensions comparable to the optical wavelength, generated using the casting and curing procedures described previously with the dot pattern masters, were placed into a conformal contact with a transparent film of a photopolymer (SU-8, MicroChem, 5–15 μm). Shining ultraviolet light through the mask, using procedures described previously,¹² generates a complex 3-D intensity distribution that exposes the photopolymer through its depth. Peeling off the mask, baking the photopolymer at 75 °C for 5–10 min to initiate cross-linking in the exposed regions, followed by a developing step to remove the uncross-linked regions completed the process. For the examples presented here, the developer was removed by drying with supercritical CO₂. The resulting three-dimensional structures have geometries defined by the intensity pattern formed by passage of light through the masks.

Plasmonic Crystal Fabrication. Solvent assisted micromolding (SAMIM) with a-PFPE molds and soft imprinting with h-PDMS molds patterned relief structures for a quasi-three-dimensional type of plasmonic crystal. Both a-PFPE/s-PDMS and h-PDMS/s-PDMS molds were cast and cured from the dot pattern masters as described previously. For the case of a-PFPE/s-PDMS, the molded layer consisted of a ~ 10 μm film of epoxy (NanoSU-8, MicroChem, formulation 10) spin cast onto a glass slide at 3000 rpm for 30 s and subsequently soft baked at 65 °C (1 min) and 95 °C (5 min). The molds were wetted with a small amount of ethanol and then placed into contact with the epoxy layer for 40 min. The ethanol softened the epoxy and caused it to flow into the surface relief of the molds. Peeling away the molds followed by exposing with a UV Hg lamp (350–380 nm) for 5 min with an intensity of 4 mW/cm² and baking at 65 °C (1 min) and 95 °C (5 min) yielded relief structures in the geometry of the molds. Since h-PDMS swells slightly with ethanol, plasmonic crystals were fabricated with h-PDMS/s-PDMS molds by soft imprint lithography on layers of polyurethane (NOA-73, Norland Optical Adhesive) as described previously.²⁸

Molecular Scale Molding. The masters consisted of randomly aligned individual SWNTs with diameters between ~ 0.6 and 3 nm and coverages of between 1 and 10 tubes/ μm^2 , grown on SiO₂/Si wafers by chemical vapor deposition using a relatively high concentration of ferritin catalyst and methane feed gas, according to procedures described previously.^{14,26} Molds (h-PDMS/s-PDMS or a-PFPE/PET) generated by casting and curing against these SWNT masters were placed against thin layers of a photocurable polymer (NOA-73) spin cast onto SiO₂/Si substrates at 9000 rpm for 40 s. Shining UV light through the molds with an Hg lamp (350–380 nm) for 2 h with an intensity of 4 mW/cm² cured the polymer. Peeling off the molds completed the process, leaving a replica of relief corresponding to the nanotubes on the polymer surfaces. These procedures followed the optimized methods described recently.^{14,26}

(28) Malyarchuk, V.; Hua, F.; Mack, N.; Velasquez, V.; White, J.; Nuzzo, R.; Rogers, J. A. *Opt. Express* **2005**, *13*, 5669–5675.

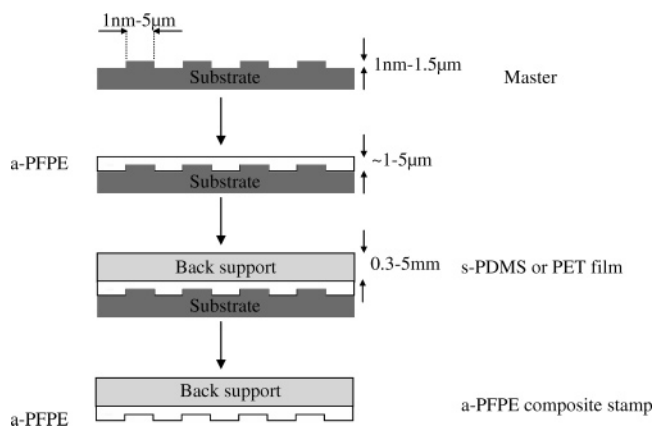


Figure 1. Schematic illustration of steps for fabricating composite a-PFPE elements as stamps, molds, and conformable phase masks. Spin casting a layer of prepolymer to a-PFPE (thickness $\sim 2 \mu\text{m}$) on a master and then curing with ultraviolet light forms a solid layer of a-PFPE with relief in the geometry defined by the master. Pouring a precursor to a low modulus PDMS ($\sim 1.5 \text{ MPa}$; s-PDMS) on this a-PFPE layer and then curing it generates a 4–5 mm thick soft backing to facilitate handling. Peeling the composite a-PFPE/s-PDMS structure away from the master yields a conformable element suitable for use in microcontact printing, nanotransfer printing, phase-shift lithography, proximity field nanopatterning, and soft imprinting. For molecular scale imprinting experiments, we used a backing layer of polyethylene terephthalate (PET) with a spin cast photocurable polyurethane adhesion layer.

We note that for the case of h-PDMS/s-PDMS molds, it was necessary to use fluorinated silanes to prevent adhesion with the underlying SiO_2 . This treatment was not necessary for a-PFPE due to its low surface energy.

Results and Discussion

Figure 1 schematically illustrates the procedures for fabricating composite a-PFPE elements. For most cases, we used a backing layer of s-PDMS, in which spin casting and photocuring a thin film of a-PFPE against the patterned surface forms the first layer of the element. The inertness of a-PFPE eliminates the necessity of treating the surfaces of the masters, particularly those with exposed oxides, with fluorinated silanes, which is often required with PDMS to prevent sticking during the casting and curing steps. Although the fluorination does not affect significantly the dimensions of features larger than a few tens of nanometers, it can be important at molecular scales, as illustrated next with the molding experiments that produce relief features with dimensions of individual SWNTs. Pouring a prepolymer of PDMS (Sylgard 184; base/initiator = 10:1 wt) on the solid a-PFPE layer and then thermally curing at room temperature for 48 h forms the PDMS backing layer ($\sim 4 \text{ mm}$ thick). This room temperature curing minimizes shrinkage of the PDMS. The low modulus s-PDMS backing layer enhances the conformal contact of the a-PFPE surface to the targets surfaces and enables in most cases good contact with little or no applied pressure. These composite a-PFPE/s-PDMS elements were used for μCP , nTP, phase-shift lithography, soft imprinting, and PnP. For molecular scale imprinting, elements with backing layers of thin ($\sim 0.3 \text{ mm}$) sheets of PET (polyethylene terephthalate) bonded to a-PFPE using a UV curable adhesive (NOA 73) yield better results than those obtained with a-PFPE/s-PDMS elements. In all of these composite designs, the strength of adhesion between the a-PFPE and the other layers, while sufficient for the soft lithographic demonstration experiments presented here, was moderate to low. Mechanical approaches, such as implementing rough surfaces, can improve the degree of adhesion.

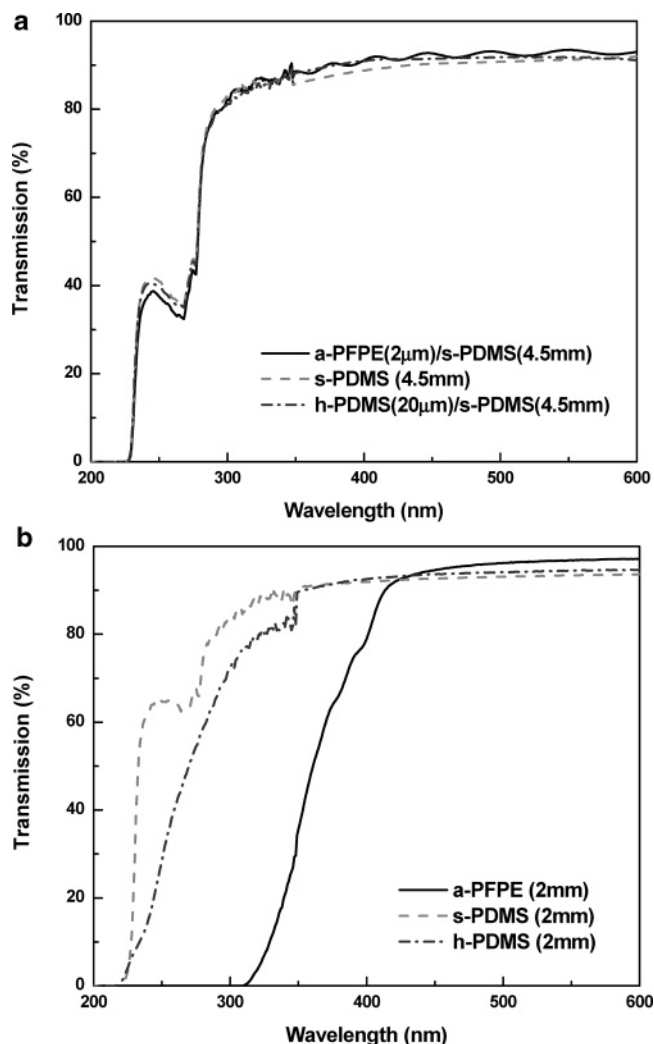


Figure 2. (a) Optical transmission spectra of s-PDMS (4.5 mm), h-PDMS($20 \mu\text{m}$)/s-PDMS(4.5 mm), and a-PFPE($2 \mu\text{m}$)/s-PDMS(4.5 mm) stamps. (b) Optical transmission spectra of s-PDMS, h-PDMS, and a-PFPE, with thicknesses of $\sim 2 \text{ mm}$.

For optical soft lithographic techniques, such as phase-shift lithography and PnP, the optical characteristics of the elastomeric masks are important. Figure 2a shows the transmission spectra of an a-PFPE ($2 \mu\text{m}$)/s-PDMS ($\sim 4.5 \text{ mm}$) composite mask, indicating transparency down to wavelengths of $\sim 300 \text{ nm}$ (the transmission is 75% at a wavelength of 300 nm), as required for phase-shift lithography and proximity field nanopatterning. In the design of the composite stamp, the a-PFPE layer is much thinner ($\sim 2 \mu\text{m}$) than the s-PDMS layer (4.5 mm), and therefore, the transmission is dominated by s-PDMS. Figure 2b shows the transmission spectrum of a-PFPE (2 mm) itself, with comparisons to s-PDMS (2 mm) and h-PDMS (2 mm). a-PFPE begins to absorb at wavelengths $\sim 100 \text{ nm}$ longer than s-PDMS or h-PDMS. The absorption of a-PFPE is most likely due to the carboxylate groups $-(\text{COO}-)$.

We first examined the properties of the patterning elements themselves. The masters for these studies consisted of arrays of cylindrical holes in a layer of a photoresist on SiO_2/Si substrates. Figure 3 shows some representative scanning electron microscope (SEM) images of composite stamps of h-PDMS ($20 \mu\text{m}$)/s-PDMS (4 mm) (Figure 3a,c,e,g) and a-PFPE ($2 \mu\text{m}$)/s-PDMS (4 mm) (Figure 3b,d,f,h). For features with diameters of 450 nm, periodicities of 750 nm (Figure 3a,b) or larger and depths of 300 nm, both a-PFPE and h-PDMS accurately replicate the features. For smaller features with the same depths, the relief on the

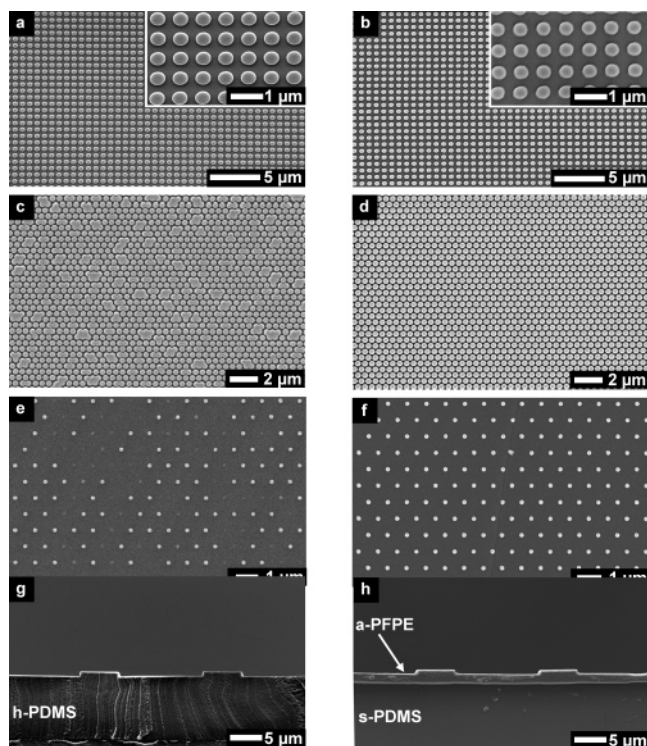


Figure 3. Scanning electron micrographs of composite elements of h-PDMS/s-PDMS (a, c, e, and g) and a-PFPE/s-PDMS (b, d, f, and h) generated by casting and curing against masters of patterned photoresistors on SiO₂/Si. Elements shown in panels a and b consist of square arrays of posts (diameter = 450 nm, periodicity = 750 nm, and relief depth = 300 nm) and were used for microcontact printing. Elements in panels c and d consist of hexagonal arrays of posts (diameter = 350 nm, periodicity = 500 nm, and relief depth = 420 nm) and were used for proximity field nanopatterning. Elements in panels e and f consist of hexagonal arrays of posts (dimension = 130 nm, periodicity = 800 nm, and relief depth = 420 nm). Frames (g and h) show cross-sectional views of elements used for phase-shift lithography (line width = 6.5 μ m, line spacing = 13.5 μ m, and relief height = 500 nm). The results suggest that a-PFPE is better able to produce, with low defects, structures that have small dimensions and large relief heights.

h-PDMS exhibits defects, in the form of merged (Figure 3c) or missing (Figure 3e) posts, neither of which are observed in a-PFPE (Figure 3d,f). The pattern of Figure 3e, which is particularly challenging for h-PDMS but not a-PFPE, consists of posts with diameters of 130 nm and heights of 420 nm, in a hexagonal array with an 800 nm periodicity. We suspect that the absence of missing posts in the a-PFPE results, at least partly, from the better release properties from the master as compared to h-PDMS, due to its comparatively lower strength of adhesion. The higher tendency of the h-PDMS posts to merge may result from its high surface energy, as compared to a-PFPE. Figure 3g,h shows cross-sectional views of a-PFPE (2 μ m)/s-PDMS (4 μ m) and h-PDMS (20 μ m)/s-PDMS (4 μ m) elements for phase-shift lithography made from an silicon-on-insulator (SOI) master with line and space patterns (line width = 13.5 μ m and line spacing = 6.5 μ m). At these length scales, both materials accurately replicate the relief structures.

Figure 4 shows results from microcontact printing with composite patterning elements similar to those shown in Figure 3 as stamps. In this process, an ethanolic solution of hexadecanethiol (HDT) inks the surface of the stamps. Contacting these inked stamps to thin film of Au forms a self-assembled monolayer in the geometry of the relief on the stamps. Etching away the unprinted regions yields patterns of Au. Both stamp materials

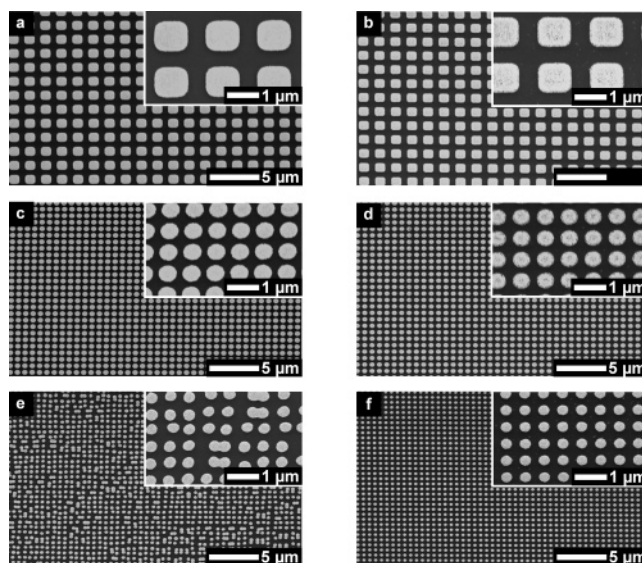


Figure 4. Scanning electron micrographs of patterns of gold generated by microcontact printing (μ CP) using h-PDMS/s-PDMS (a, c, and e) and a-PFPE/PDMS stamps (b, d, and f). The patterns on the masters had periodicities of 1.6 μ m (a and b), 750 nm (c and d), and 600 nm (e and f); diameters of 970 nm (a and b), 450 nm (c and d), and 260 nm (e and f); and depths of 300 nm.

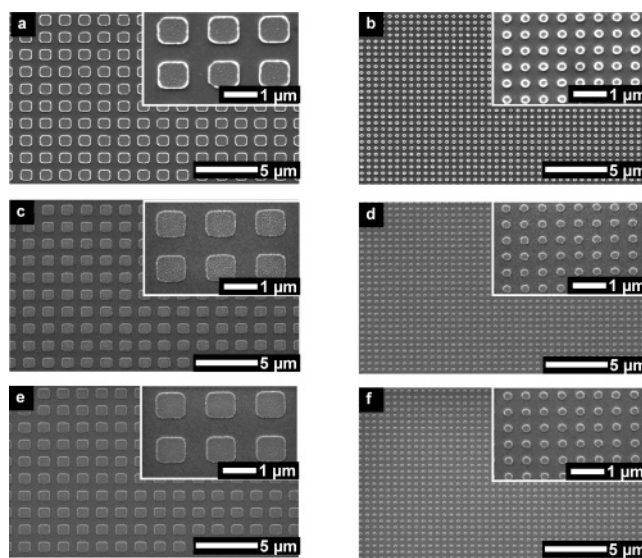


Figure 5. Scanning electron micrographs of patterns generated by nanotransfer printing (nTP) using Ti/Au (2 nm/20 nm) on h-PDMS/s-PDMS (a and b); Ti/Au (2 nm/20 nm) on a-PFPE/s-PDMS (c and d); and Ti/Au/Ti/Au (8 nm/10 nm/2 nm/10 nm) on a-PFPE/s-PDMS. The patterns on the masters have diameters of 970 nm (a, c, and e) and 260 nm (b, d, and f), periodicities of 1.6 μ m (a, c, and e) and 600 nm (b, d, and f), and depths of 300 nm.

offer excellent printing results for 970 nm diameter dots with a periodicity of 1.6 μ m (Figure 4a,b) and for 450 nm diameter dots with a periodicity of 750 nm (Figure 4c,d). The a-PFPE/s-PDMS stamps show better performance than h-PDMS/s-PDMS for 260 nm dots (Figure 4e,f), due to the better replication of a-PFPE as illustrated in Figure 3. The defects observed in the smallest printed features (Figure 4e) using the h-PDMS stamp result from merging defects in the stamps, as illustrated in Figure 3. We find that a-PFPE requires longer inking times (5–10 min) as compared to h-PDMS (30 s), suggesting that the uptake of the ink into the a-PFPE is less, for a given time, than h-PDMS. Furthermore, contact times needed to yield defect free patterns in the etched gold are found to be somewhat longer for a-PFPE (~30 s), as

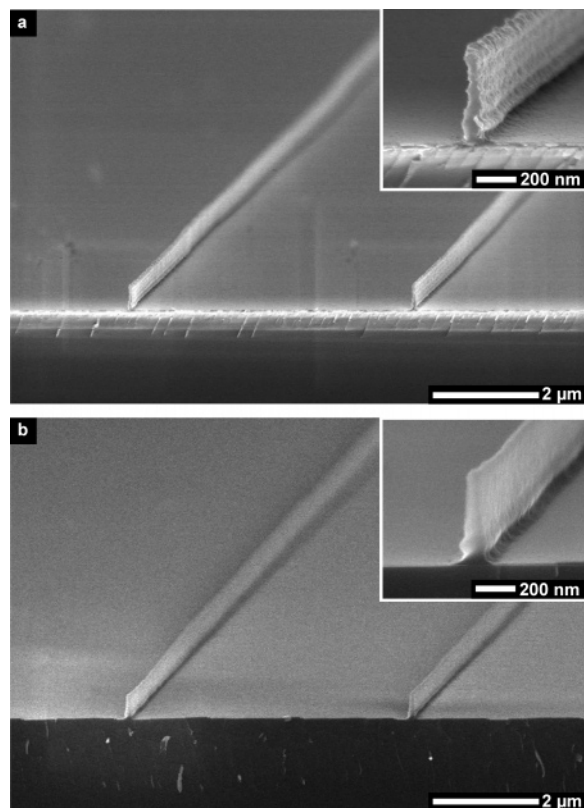


Figure 6. Scanning electron micrographs of line patterns in photoresists generated using (a) h-PDMS/s-PDMS and (b) a-PFPE/s-PDMS phase-shift masks. The line spacing is $5 \mu\text{m}$, and the widths are $\sim 100 \text{ nm}$. The insets provide cross-sectional magnified views.

compared to h-PDMS ($\sim 5 \text{ s}$). This observation is likely related to the different inking behaviors and to conformal contact that tends to happen more readily with h-PDMS than with a-PFPE.

The same types of composite stamps can be used to pattern gold by nanotransfer printing (nTP). In this approach, gold deposited onto a stamp is transferred to a target substrate via one of a variety of mechanisms, such as cold welding to a thin layer of gold on the target substrate.²⁴ Optimized conditions for printing with PDMS involve a short oxygen plasma treatment and a thin layer of titanium to minimize nanoscale cracks that can form during evaporation of gold onto the PDMS.²⁴ Figure 5a,b shows patterns of Ti/Au (2 nm/20 nm) printed using such procedures with a h-PDMS/s-PDMS stamp. Some ultrathin residue of PDMS can be left on the printed structures, due to the relatively good bonding between the oxygen plasma treated PDMS and the Ti/Au bilayer. This PDMS can be removed by a plasma treatment with oxygen and tetrafluoromethane, as described previously.²⁴ These optimized conditions do not apply to a-PFPE/s-PDMS stamps, due to their different surface chemistries. Although there are nanocracks present in the patterns transferred from a-PFPE/s-PDMS stamps, as shown in Figure 5c,d, the transfer efficiency is extremely high, due to the very poor adhesion of the metal (Ti/Au, 2 nm/20 nm) to the a-PFPE. Multilayer stacks of metals (Ti/Au/Ti/Au, 8 nm/10 nm/2 nm/10 nm) can generate patterns with minimal cracking at high yield, as illustrated in Figure 5e,f.

Figure 6 compares the operation of a-PFPE and h-PDMS based phase-shift masks for patterning $\sim 100 \text{ nm}$ features in photoresists. Phase masks fabricated from SOI masters (line ($13.5 \mu\text{m}$) and space ($6.5 \mu\text{m}$) pattern) provide well-controlled geometry with sharp, vertical sidewalls as shown in Figure 3. The patterning process involves exposing a thin layer of a photoresist ($\sim 500 \text{ nm}$, Shipley 1805 spin cast at 3000 rpm for 30s) by shining UV

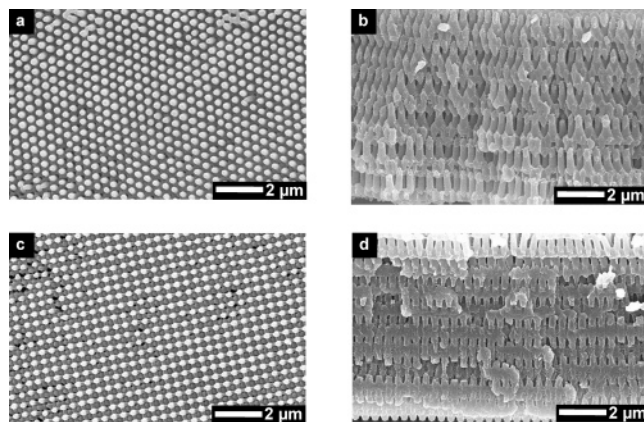


Figure 7. Top (a) and cross-sectional (b) SEM images of 3-D nanostructures generated with a-PFPE/s-PDMS phase masks with relief in the geometry posts in hexagonal arrays, with diameters, periodicities, and heights of 350, 500, and 420 nm, respectively. Panels c and d provide top and cross-sectional views, respectively, of 3-D nanostructures generated by a-PFPE/s-PDMS masks with relief in the geometry posts in a square array, with diameters, periodicities, and heights of 280, 400, and 420 nm, respectively.

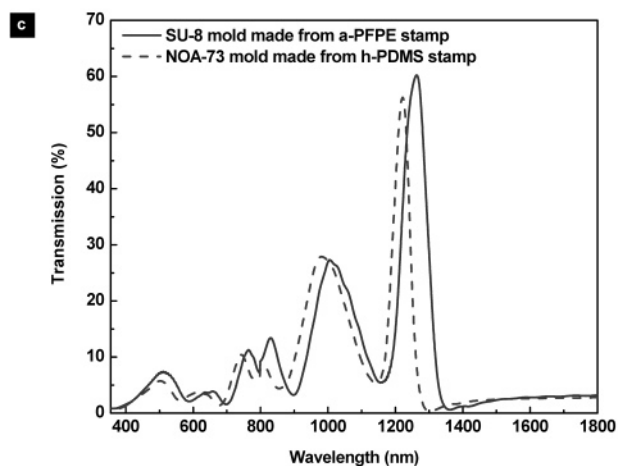
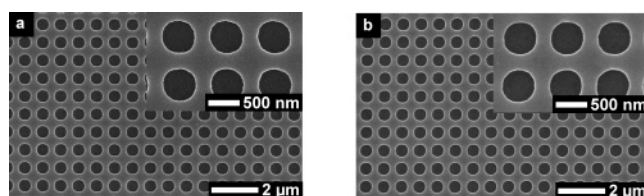


Figure 8. SEM images of plasmonic crystals formed using gold coated (a) photurable polyurethane imprinted with an h-PDMS mold (diameter = 480, periodicity = 780 nm, and relief depth = 400 nm) and (b) epoxy molded by SAMIM using an a-PFPE mold. Panel c shows the normal incidence transmission spectra of these plasmonic structures. The spectral shifts are likely due to differences in the index of polyurethane and epoxy.

light through a phase mask while it was in conformal contact with the photoresist. This contact, which is driven by generalized adhesion forces,^{7–9} places the photoresist in the near field region of the mask. Optical phase-shifting effects at the step edges produce local reductions in the intensity of UV light in these regions. Postexposure development produces lines of the positive photoresist. The behavior of phase-shift masks made of a-PFPE ($2 \mu\text{m}$)/s-PDMS (4 mm) in this process is indistinguishable from that of masks of h-PDMS ($20 \mu\text{m}$)/s-PDMS (4 mm). In particular,

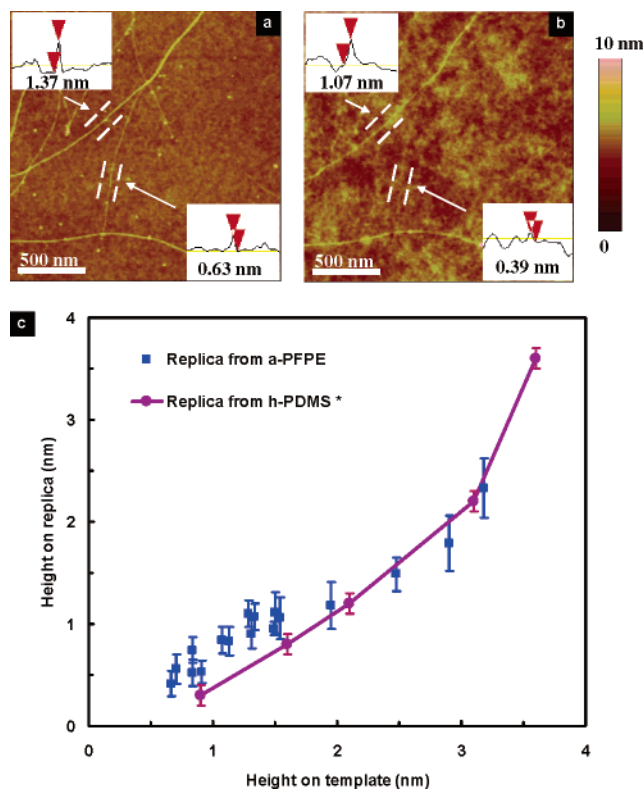


Figure 9. Molecular scale imprinting using single walled carbon nanotubes (SWNTs) as masters. (a) Atomic force microscopic (AFM) image of a representative region of a master (random SWNTs on SiO₂/Si). (b) AFM image of the relief structure on a layer of polyurethane imprinted with an a-PFPE/s-PDMS mold. (c) Comparison of relief height replication using h-PDMS and a-PFPE molds. The relief height replication fidelity using a-PFPE is slightly better than h-PDMS for nanotubes with sizes less than ~ 1.5 nm. (Data for relief height replication with h-PDMS are adapted from Hua.²⁶)

lines of the photoresist with widths and heights of ~ 100 and ~ 500 nm, respectively, can be fabricated in both cases, as shown in Figure 6.

Such phase masks can also be used, with transparent photopolymers, to produce three-dimensional nanostructures in a single exposure step, using a process known as PnP. Figure 7a,b show structures of an epoxy (SU8, Microchem Corp.) photoexposed through an a-PFPE/s-PDMS mask with relief in the form of hexagonal arrays of posts with diameters, periodicities, and heights of 350, 500, and 420 nm, respectively. Figure 7c,d shows three-dimensional structures made from a-PFPE/s-PDMS masks with smaller posts (diameter = 280 nm and periodicity = 400 nm). These structure geometries are consistent with expectations based on modeling of the optics. It was impossible to generate masks with these geometries using h-PDMS due to the relatively high density of merged and missing posts, as illustrated in Figure 3. The capability of a-PFPE to produce defect-free phase masks in this range of feature sizes enables new opportunities in three-dimensional nanofabrication with PnP.

In a final set of experiments, we compared a-PFPE to h-PDMS for soft imprinting. In a first example, we used molds with geometries similar to those shown in Figure 3 to create relief structures for a type of quasi-three-dimensional plasmonic crystal device. Figure 8a,b shows SEM images of such plasmonic crystals formed by electron beam evaporation of thin films of gold (50 nm) onto structures of relief fabricated using h-PDMS/s-PDMS and a-PFPE/s-PDMS molds. The patterns in these cases correspond to square arrays of 480 nm diameter holes with a periodicity of 780 nm and a depth of 400 nm. The crystals formed

with h-PDMS (Figure 8a) use photocurable polyurethane (NOA-73) patterned according to procedures described previously.²⁸ Samples generated with a-PFPE (Figure 8b) used solvent assisted micromolding (SAMIM) of a thin layer of epoxy (SU-8, Microchem Corp.). (Molding of polyurethane (NOA-73) with the a-PFPE/s-PDMS composite stamps tended to lead to bonding failure at the interface of a-PFPE and s-PDMS upon releasing of the stamp after curing the polyurethane.) The SEM images of Figure 8a,b show that structures formed using these two approaches have a similar appearance. The normal incidence transmission spectra, as shown in Figure 8c, are important for sensing applications.²⁹ The general features of spectra are similar, with an overall spectral shift that is due, at least in part, to the difference in index of refraction between the NOA-73 (1.56) and the SU-8 (1.58–1.67). The possible change in periodicity of the structures on polyurethane and epoxy due to the differences in shrinkage of h-PDMS and a-PFPE could also be important for the spectral shift. By comparing the changes in periodicity of line and space patterns replicated with an a-PFPE/s-PDMS stamp and with h-PDMS/s-PDMS, we determined that the shrinkage of a-PFPE ($0.6 \pm 0.2\%$) is comparable to that of h-PDMS ($0.7 \pm 0.2\%$).

The ultimate resolution in soft imprinting can be evaluated using single walled carbon nanotubes (SWNTs) as masters.^{14,26} Recent studies show that this type of molding procedure can provide a resolution approaching 1 nm, using h-PDMS/s-PDMS molds and optimized procedures.^{14,26} We demonstrate in this work that a-PFPE can provide a comparable resolution. Figure 9a presents an AFM image ($2 \mu\text{m} \times 2 \mu\text{m}$) of a representative region of SWNTs on a SiO₂/Si substrate that served as a master. The range of diameters in such SWNTs and the atomic scale uniformity in their diameters over lengths of tens of micrometers are ideal for investigating resolution at the molecular scale. Figure 9b shows an AFM image of a layer of polyurethane (PU) molded using a composite a-PFPE/PET mold formed by casting and curing against the SWNT master. The results indicate that SWNTs with diameters as small as ~ 0.6 nm can be replicated, to some extent, by a-PFPE. The surface roughness in the molded layers limits the replication fidelity at these scales. Detailed AFM measurement shows that the surface roughness of a replica (PU) from the a-PFPE mold is between 0.4 and 0.5 nm, slightly higher than replicas formed using h-PDMS molds (as small as ~ 0.3 nm). On the other hand, statistical analysis of molded features, as shown in Figure 9c, suggests that a-PFPE enables more accurate replication of feature heights, as compared to h-PDMS, in the ~ 1 nm range. One possible reason for this difference is that the master for a-PFPE was not treated with fluorinated silanes, unlike the case for PDMS. The thickness of this fluorinated silane layer could reduce, especially at the ~ 1 nm scale, the replicated relief depth as compared to the dimensions of the SWNTs.

Conclusion

In summary, we have compared a commercially available formulation of perfluoropolyether polymer (a-PFPE) with h-PDMS for use in a variety of soft lithographic techniques including microcontact printing, nanotransfer printing, phase-shift optical lithography, proximity field nanopatterning, molecular scale soft nanoimprinting, and solvent assisted micromolding. The a-PFPE material, in the form of composite stamps, appears to hold promise as an alternative to PDMS for certain soft lithographic methods, due mainly to its capability of high fidelity replication and chemical inertness. In several cases, however, the intrinsic differences in the chemistries of a-PFPE and PDMS make it necessary to

(29) Stewart, M. E.; Mack, N. H.; Malyarchuk, V.; Soares, J. A. N. T.; Lee, T.-W.; Grayd, S. K.; Nuzzo, R. G.; Rogers, J. A. *Proc. Natl. Acad. Sci. U.S.A.* **2006**, *103*, 17143–17148.

re-examine the processing conditions. For instance, the chemical inertness and low surface energy of a-PFPE eliminate the need to functionalize the surfaces of oxides on masters, but these same properties lead to longer inking and contacting times in microcontact printing. Through careful optimization, a-PFPE can be an excellent material for soft lithography, for a variety of applications including electronics, microfluidics, and biosensing.

Acknowledgment. This work is supported by the NSF through Grants DMI 03-55532 and the Center for Nanoscale Chemical Electrical Mechanical Manufacturing Systems at the University

of Illinois, which is funded by the NSF under Grant DMI-0328162. We also received funding from Frederick Seitz Materials Research Laboratory, University of Illinois, which is partially supported by the U.S. Department of Energy under Grant DEFG02-91-ER45439. Use of the Center for Nanoscale Materials was supported by the U.S. Department of Energy, Office of Science, Office of Basic Energy Sciences, under Contract W-31-109-Eng-38. T.T.T. gratefully acknowledges a graduate fellowship from the Vietnam Education Foundation.

LA062981K